DOI: 10.1002/ejic.200800349

Synthesis and Characterization of Linear Trinuclear Pd, Co, and Pd/Co Pyrazolate Complexes

Haralampos N. Miras,[a] Hong Zhao,[a] Radovan Herchel,[b] Carlos Rinaldi,[c] Soribel Pérez,[a] and Raphael G. Raptis*[a]

Keywords: Heterometallic compounds / Nitrogen heterocycles / Magnetic properties / Palladium / Cobalt

A family of dinuclear and linear trinuclear Co/Pd pyrazolate compounds, namely, $[Bu_4N]_2[Co_2(\mu\text{-}4\text{-}Cl\text{-}3,5\text{-}Me_2\text{-}pz)_2Cl_4]$ (**1**), $[Bu_4N]_2[Co_2(\mu\text{-}4\text{-}Br\text{-}3,5\text{-}Me_2\text{-}pz)_2Br_4]$ (**2**), $[Bu_4N]_2[Co_2(4\text{-}I\text{-}3,5\text{-}Me_2\text{-}pz)_2Cl_4]$ (**3**), $[Et_4N]_2[Pd_2Co(4\text{-}Br\text{-}3,5\text{-}Me_2\text{-}pz)_4Cl_4]$ (**4**), $[Et_3NH]_4[PdCo_2(4\text{-}Br\text{-}3,5\text{-}Me_2\text{-}pz)_4Cl_4][NO_3]_2$ (**5**), $[Et_3NH]_2[Pd\ Co_2(3\text{-}Me\text{-}5\text{-}Ph\text{-}pz)_4Cl_4]$ (**6**), $[Et_3NH]_2[Pd_3(4\text{-}Br\text{-}3,5\text{-}Me_2\text{-}pz)_4Cl_4]$ (**7**), and $[Co_3(3,5\text{-}Me_2\text{-}pz)_4(3,5\text{-}Me_2\text{-}pzH)_2(CH_3CO_2)_2]$ (**8**) was synthesized. The single-phase nature of the solids was established by single-crystal X-ray diffraction, thermal analysis, and spectroscopic techniques. Moreover, the magnetic behavior is studied and a magnetostructural comparison to the corresponding carboxylate analogues is made.

Introduction

This work stems from our interest in exploring the structural parallel between transition-metal pyrazolate and carboxylate chemistry.[1] Polynuclear transition-metal carboxylate complexes have been widely investigated for the following reasons: (i) Besides 1D, 2D, or 3D magnetic ordering,[2–5] it has been shown that carboxylate complexes show single-molecule magnet (SMM) properties. (ii) Several carboxylate complexes have been successfully used as biomimetic models of metalloprotein polynuclear active centers.[5d,5e] (iii) Metal carboxylates can be viewed as extended models of intermediates during the formation of geological sediments.[5f] (iv) A variety of unique organic reactions are efficiently catalyzed by polynuclear carboxylates due to the ability of polymetallic centers to coordinate and to activate several functional groups of a substrate.[5e,5g] (v) It has recently been demonstrated that polynuclear carboxylate complexes can be used as precursors for the preparation of nanosized magnetic oxide particles.[6–8]

The synthesis and structural characterization of carboxylato-bridged complexes is now a well-developed field.[2–10] In our previously reported work we suggested that a wide class of polynuclear metal–pyrazolates with interesting redox and magnetic properties, which are structural analogues of known carboxylates of the same metals, remain to be fully explored.[1] Evidently, the field of metal–pyrazolates is significantly less developed than that of the analogous carboxylates.[9] Still, several oligonuclear metallocyclic pyrazolato complexes, from tri- to tetradecanuclear, are known.[1b,11–14] In contrast, only a limited number of noncyclic metal–pyrazolate structural motifs have been reported so far.[11,12d,15]

Studies of the exchange interaction between paramagnetic metal centers through multiatom bridging ligands are important to a variety of research areas, ranging from coordination chemistry to solid-state physics, biology, and bioinorganic chemistry.[16–30] Chauduri et al., as well as others, have reported extensively on the exchange interactions between paramagnetic metal centers bridged by three-atom bridges in di- and trinuclear, homo- and heterometallic complexes.[16–18,21–30] Analogous studies of systems involving pyrazolate bridges have been hitherto lacking.

Here we report the first part of our studies of linear trinuclear pyrazolato complexes, involving homometallic (Pd or Co) and heterobimetallic (Pd/Co) systems, including the syntheses, magnetic, thermal, spectroscopic, and X-ray structural characterization of $[Bu_4N]_2[Co_2(4\text{-}Cl\text{-}3,5\text{-}Me_2\text{-}pz)_2Cl_4]$ (**1**), $[Bu_4N]_2[Co_2(4\text{-}Br\text{-}3,5\text{-}Me_2\text{-}pz)_2Br_4]$ (**2**), $[Bu_4N]_2[Co_2(4\text{-}I\text{-}3,5\text{-}Me_2\text{-}pz)_2Cl_4]$ (**3**), $[Et_4N]_2[Pd_2Co(4\text{-}Br\text{-}3,5\text{-}Me_2\text{-}pz)_4Cl_4]$ (**4**), $[Et_3NH]_4[PdCo_2(4\text{-}Br\text{-}3,5\text{-}Me_2\text{-}pz)_4Cl_4][NO_3]_2$ (**5**), $[Et_3NH]_2[PdCo_2(3\text{-}Me\text{-}5\text{-}Ph\text{-}pz)_4Cl_4]$ (**6**), $[Et_3NH]_2[Pd_3(4\text{-}Br\text{-}3,5\text{-}Me_2\text{-}pz)_4Cl_4]$ (**7**), and $[Co_3(3,5\text{-}Me_2\text{-}pz)_4(3,5\text{-}Me_2\text{-}pzH)_2(CH_3CO_2)_2]$ (**8**), where 4-X-3,5-Me_2-pzH and 4-X-3,5-Me_2-pz represent the ligands 4-X-3,5-dimethylpyrazole and 4-X-3,5-dimethylpyrazolate anion (X = Cl, Br, I).

[a] Department of Chemistry and the Institute of Functional Nanomaterials, University of Puerto Rico, San Juan, PR 00931-3346, USA
E-mail: raphael@adam.uprr.pr
[b] Department of Inorganic Chemistry, Palacký University, Křížkovského 10, CZ-77147 Olomouc, Czech Republic.
[c] Department of Chemical Engineering and the Institute of Functional Nanomaterials, University of Puerto Rico, Mayagüez, PR 00681-9046, USA

Results and Discussion

Syntheses

A straightforward, clean and of relatively good yield synthetic route to dinuclear and linear trinuclear complexes incorporating 3,5-disubstituted or 3,4,5-trisubstituted pyrazolate bridges has been developed, as outlined in Scheme 1. Dinuclear complexes **1**–**3** were isolated from simple reactions of Co^{II} halides with the appropriate pyrazole and triethylamine in thf solutions. The role of triethylamine was to deprotonate the pyrazoles, but triethylammonium cations also served as counterions in the crystal lattices of compounds **5**–**7**. The 4-position of coordinated pyrazole ligands is often halogenated during reactions involving halides.[31] The use of 4-halogen-substituted pyrazoles here was to avoid such partial halogenation, which would make difficult the accurate molecular weight determination of the products, creating in turn a problem in the analysis of magnetic susceptibility data. Mononuclear or Co/Pd dinuclear species, which may exist in reaction mixtures involving both Co and Pd starting materials, have not been isolated in the solid state. Instead, trinuclear heterobimetallic complexes **4**–**6**, containing at least one Co^{II} as the terminal metal center, were the only crystalline species isolated from such one-pot reactions. Similar chemistry has been reported in carboxylate systems.[5c] According to the latter study, an interconversion between a dinuclear and *cyclic* trinuclear Co–carboxylate species takes place, triggered by counterion effects and reaction conditions.

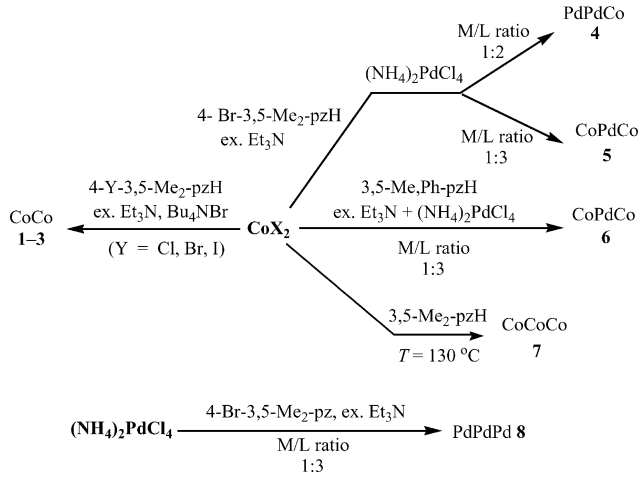

Scheme 1. Synthetic routes leading to the isolation of **1**–**8**.

Anionic heterotrinuclear species **4**–**6** were isolated upon addition of $(NH_4)_2PdCl_4$ to a thf solution of CoX_2 (X = Cl^- and NO_3^-) and 4-Br-3,5-Me_2-pzH, followed by overnight reflux. The lability of Co^{II} cations in combination with the relative kinetic inertness of Pd^{II} (compared to Co^{II}) cations and the preference of the bridging agent to coordinate with a softer acid, induced the isolation of PdPdCo **4** and CoPdCo **5** and **6** species through one-pot reaction processes.

Two noteworthy features were derived from the above observations: (i) The cobalt metal centers retain their oxidation state of (II), although the solution was heated at reflux overnight in air, as well as adopt a tetrahedral geometry, in contrast to analogous reactions involving carboxylate ligands.[25,26,28] (ii) The Co/Pd ratio in the reaction mixture was not a determining factor of the nature of the isolated species. Only in the case where the Co/Pd ratio exceeded the proportion of 1:3.5, then the isolated product was Co/Pd-ratio-dependent and the final product was a palladium dimer and/or polymer. It is established that the pyrazolate ligands favored the isolation of linear trinuclear species, in contrast with carboxylate analogue system under the same experimental conditions.[27]

In the absence of Co^{II} species in a thf solution after overnight reflux, trinuclear linear palladium compound **7** was isolated in quite good yield. In this case, the bridging ligand is available only for the Pd^{II} metal centers, avoiding the coexistence of equilibrium byproducts and making the isolation procedure straightforward if the ligand-to-metal ratio is equal or higher than 3.

In our effort to isolate homonuclear trinuclear cobalt analogue **8**, we envisaged a different route avoiding the formation of polymer insoluble products. Reaction, in the solid state, of cobalt acetate in the presence of the bridging agent by applying high temperatures (130 °C) and dissolution of the paste in CH_2Cl_2 gave the desirable product. Also, in this case, Co^{II} retained its oxidation state and geometry.

X-ray Crystallography

A selection of interatomic distances and bond angles relevant to the cobalt and palladium coordination spheres for compounds **1**–**8** are listed in Tables 1–5.

X-ray structural analysis of compounds **1**–**3** revealed the presence of the dimer unit $[Co_2(4\text{-X-}3,5\text{-}Me_2\text{-pz})_2Cl_4]^{2-}$ (X: Cl, Br, I, Figure 1) as well as two Bu_4N^+ counterions. The Co^{II} centers are held together by two 4-X-3,5-Me_2-pz bridges at a distance of 3.707(9)–3.7355(7) Å [the dihedral angles between pyrazolate planes are 174.8(1)–175.8(8)°] and much longer than the Co–carboxylate analogues,[5c] where the metal centers are separated by distances of 3.028(1) and 3.550(5) Å, respectively. The Co–N distances range from 1.979(9) to 2.042(9) Å, whereas four terminal Br atoms are located at a distance of 2.4084(7)–2.424(7) Å. Each cobalt metal center adopts a distorted tetrahedral geometry with angles of 104.7(1)–112.9(4)°.

Compounds **4**–**6** have linear trinuclear structures. Specifically, the structure of compound **4** consists of a discrete heteronuclear $[Pd_2Co(4\text{-Br-}3,5\text{-}Me_2\text{-pz})_4Cl_4]^{2-}$ unit (Figure 2) and two Et_3NH^+ counterions. The X-ray structure of **4** shows that a linear trinuclear compound, Co–Pd–Pd 177.96(5)°, comprising two Pd atoms with approximately square-planar geometry [the angles range from 87.3(1) to 90.5(4)°], whereas the Co center adopts a distorted tetrahedral geometry with angles ranging from 95.6(5) to 116.3(4)°. One cobalt and two palladium atoms are bridged

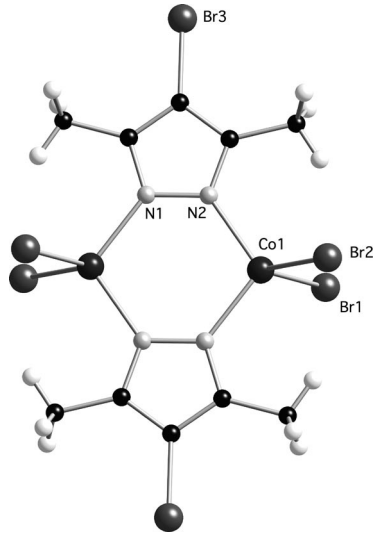

Figure 1. Ball-and-stick representation of compound **2**.

through two 4-Br-3,5-Me_2-pz bridges, whereas four chlorine atoms complete the coordination sphere of the terminal metal centers. The average Pd–$N_{(av)}$ bond length is 2.01(1) Å, in accord with previously reported Pd compounds,[1b] whereas the Co–$N_{(av)}$ bond is 2.01(1) Å long. X-ray structural data revealed a Co–$Pd_{(t)}$ distance of 6.736(2) Å, which is significantly shorter in comparison with the corresponding distance in CuPdCu [6.846(2) Å] and CrZnCr [7.140(4) Å] compounds,[20e,24] confirming our original thought of potential control of pyrazolate bridges on the distance of the terminal metal centers and potentially on the exchange coupling.

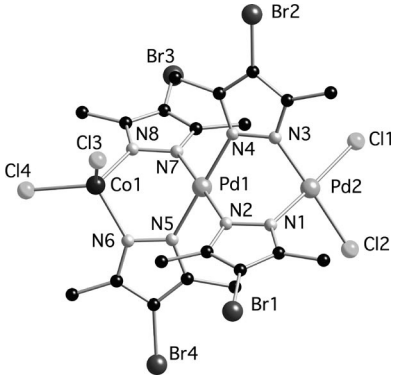

Figure 2. Ball-and-stick representation of compound **4**.

Compounds **5** and **6** present linear trinuclear structural motifs, similar to compound **4**, where a terminal Pd center is replaced by a Co atom (Figures 3 and 4). The structural features of the above-mentioned compounds were found to be similar, even though some steric hindrance was introduced by the use of the bulkier 3-Me-5-Ph-pz moiety, instead of the 4-Br-3,5-Me_2-pz unit, in the case of compound **6**. The X-ray structural analysis confirmed the isolation of centrosymmetric linear trinuclear species (Co–Pd–Co 180.00°), in both cases, where two cobalt metal centers exhibit distorted tetrahedral geometries [angles range from 99.6(2) to 116.1(1)° and from 103.8(2) to 114.82(9)° for compounds **5** and **6**, respectively], whereas the palladium metal center adopts an ideal square-planar geometry with angles ranging from 89.0(1) to 90.9(1)° and from 89.7(2) to 90.3(2)°, respectively. One palladium and two cobalt atoms are bridged together through four pyrazolate bridges, whereas four chlorine atoms complete the coordination sphere of the terminal metal centers. The average Pd–$N_{(av)}$ bond lengths are 2.016(4) Å (for **5**) and 2.017(6) Å (for **6**), whereas in the case of Co–$N_{(av)}$ the bond lengths are 2.005(5) Å and 2.033(6) Å, respectively, in good agreement with compound **4**, as well as with previously reported examples by our group.[1,12] The two terminal cobalt atoms are separated by a distance of 6.829(2) and 6.853(2) Å, for **5** and **6**, respectively, slightly longer than that in the Co–Pd–Pd **4** analogue, but still significantly shorter than that in the previously reported carboxylates. In the latter case, the terminal Co centers were separated by a distance of 6.930(3) to 7.120(2) Å.[4d,5] The same is also valid in the case of reported isostructural species with different bridging ligands,[20e,24] even though our compounds incorporate metal atoms of bigger atomic radii. In the case of carboxylate-bridged analogues, the Co^{II} metal centers are separated by longer distances, which is in agreement with the bigger and more flexible carboxy-binding angle in contrast to pyrazolate-bridged adducts.

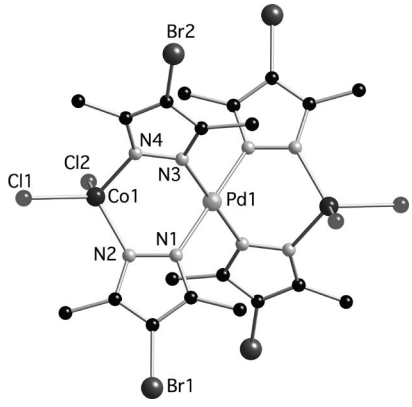

Figure 3. Ball-and-stick representation of compound **5**.

The molecular geometry and the atom labeling scheme of anionic species **7** are shown in Figure 5. The structure of the complex ion consists of a trinuclear, crystallographically centrosymmetric unit and two Et_3NH^+ cations. The X-ray structure analysis confirmed that a linear trinuclear complex, Pd–Pd–Pd 180.00°, was formed in such a way that square-planar geometry containing three Pd^{II} as central ions is present in the lattice. The metal centers are bridged together through four pyrazolate bridges, whereas the coordination sphere of the terminal palladium ions is completed by four coordinated chlorine atoms.

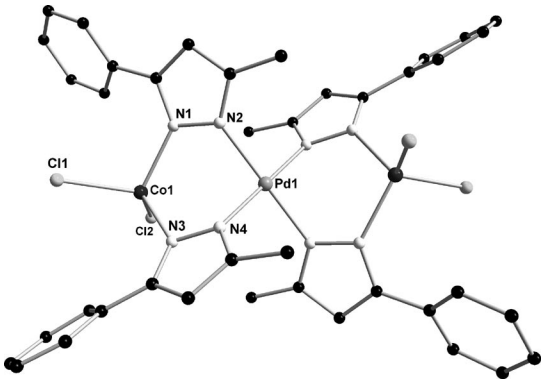

Figure 4. Ball-and-stick representation of compound **6**.

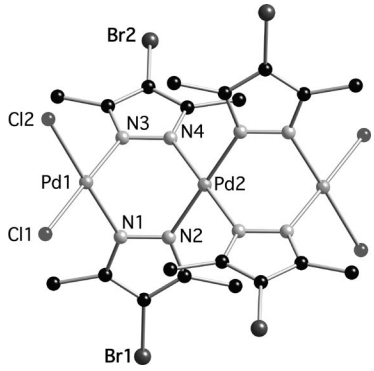

Figure 5. Ball-and-stick representation of compound **7**.

The palladium metal centers lie approximately 2° far from the ideal square-planar geometry with the Pd–N–X (X = N, Cl) angles ranging from 87.9(2) to 92.0(1)°. The Pd–$N_{(av)}$ bond length is 2.013(5) Å, which is in agreement with the previous reported compounds by our group,[1b] whereas the two terminal palladium metal centers are separated by a distance of 6.669(1) Å, which is the shortest one in this family of trinuclear species.

X-ray structural analysis of **8** revealed the presence of the homotrinuclear species $[Co_3(3,5\text{-}Me_2\text{-}pz)_4(3,5\text{-}Me_2\text{-}pzH)_2(CH_3CO_2)_2]$ (Figure 6). The latter neutral compound, which deviates from linearity by 10.9° [Co–Co–Co 169.10(2)°], consists of three cobalt atoms in distorted tetrahedral geometry [angles range from 99.5(2) to 121.3(2)°] connected together through four pyrazolate bridges, whereas the two terminal metal centers are coordinated further with one pyrazole (Me_2-pzH) and one acetate each. The average Co–$N_{(av)}$ bond length is 2.000(4) Å and in agreement with the respective ones reported above for compounds **1**–**6**. The two terminal cobalt atoms are separated by a distance of 7.177(1) Å, significantly elongated in comparison with the above-discussed distance in the case of compounds **4**–**6**, although the molecule is to some extent bent and, interestingly, in this case, similar to the carboxylate reported analogues with comparable structural motifs.[25,4d,5]

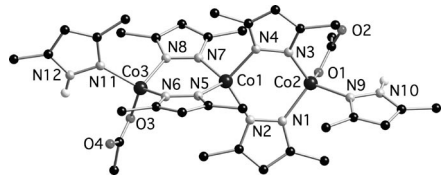

Figure 6. Ball-and-stick representation of compound **8**.

Unexpectedly, the $Co_1\cdots Co_2$ separation of 3.601(1) Å is significantly shorter than the $Co(pz)_2$ polymer structure reported by Sironi et al.,[14c,15] where the metal centers are separated by a distance of 3.7165(3) Å even though the Co–$N_{(av)}$ distance is almost identical and equal to 2.006(3) Å.

Infrared Spectra

Discussion of the IR absorptions is confined to the most important vibrations in the 4000–400 cm^{-1} region. Compounds **1**–**3** and **4**–**8** exhibit a strong doublet in the 2880–2980 cm^{-1} region indicative of the Bu_4N^+ and Et_3NH^+ cations.

The M–Cl (M = Co, Pd) stretching vibration is assigned to the medium-to-strong band at 446–462 cm^{-1}, in agreement with earlier reported work,[32] and the absence of the latter from the IR spectrum of the free pyrazole. The complex IR patterns in the 500–1800 cm^{-1} region are quite similar to the respective ones of the free ligand, but shifted to lower values upon coordination of the pyrazole to the metal centers. The absence of an NH stretching and bending vibration was observed in the IR spectra of the dinuclear complexes, indicative of the deprotonation of the ligand, something which is not consistent in the case of the trinuclear ones because of superposition with the bands of the same group originating from the counterions.

Electronic Spectra

The absorption (CH_2Cl_2 solution) and diffuse reflectance spectra of all compounds have been recorded in the ranges 200–1500 nm and 200–800 nm, respectively.

The solution and solid-state spectra of each compound are identical, indicating that the solid-state structures persist in solution. Dinuclear species **1**–**3** exhibit the highest energy spin-allowed transition of the tetrahedral Co^{II} center [$^4A_2 \rightarrow {}^4T_1(P)$]. Bands are observed at 562, 610, and 639 nm for **1**, **2**, and **3**, respectively, with extinction coefficients ranging from 300–1700 $M^{-1}cm^{-1}$, in agreement with the nature and oxidation state of the metal centers.[33]

Accordingly, compounds **4**–**6** showed a similar behavior, exhibiting the same Co^{II}-centered d–d transition at similar energies: 516, 615, and 643 nm, respectively, with extinction coefficients ranging from 1000–2100 $M^{-1}cm^{-1}$, whereas compound **8** presented transitions shifted towards the visible region, namely, 554 (sh.), 571, and 583 nm, with extinction coefficients ranging from 350–1200 $M^{-1}cm^{-1}$. In all cases a band of low intensity and $\varepsilon_M \approx 170\ M^{-1}cm^{-1}$ at

1200–1340 nm was observed and is assigned to the orbitally forbidden $^4A_2 \rightarrow {}^4T_2$ transition. Deviation from tetrahedral geometry to approximate C_{2v} symmetry causes splitting of each of the three excited states into three nondegenerate states. More specifically, in distorted tetrahedral environments, the low symmetry splitting of the $^4T_1(P)$ level results in a splitting of the $^4A_2 \rightarrow {}^4T_1(P)$ absorption envelope that provides a qualitative indication of the deviation from tetrahedral symmetry. Detailed interpretations of Co^{II} electronic spectra are complicated by the effects of the low symmetry ligand field in addition to spin–orbit coupling, Jahn–Teller effects, and the possibility of spin-forbidden transitions.[34] In many cases, the visible region of the spectra is uninformative due to the above-mentioned transitions occurring in the same region, and acquiring some intensity by means of spin–orbit coupling.[25,26,33] However, the main d–d absorption bands for these compounds all lie in the region 500–600 nm, according to other reported examples.[35]

Thermogravimetric (TG) Analyses

The TG curve of compounds **1**–**3** proved to be quite similar and only that of compound **1** is reported here. The diagram revealed an overall weight loss of 68.02% (calcd. 67.49%) in two overlapping steps up to 595.0 °C. In the first stage, a weight loss of 35.47% (calcd. 35.00%) at 142.0 °C, which is attributed to an exothermic elimination of two Bu_4N^+ counterions, is observed. The decomposition of two pyrazolate anions took place in an endothermic stage up to 595.0 °C and a weight loss of 32.55% (32.49%) has occurred.

The TGA study of compound **4** showed a total weight loss of 79.10% (calcd. 80.26%). The sample lost its initial weight in three overlapping steps at 136.0, 227.0, and 530.0 °C. Up to 136.0 °C, a weight loss of 17.53% (calcd. 18.87%) is attributed to the loss of two Et_4N^+ cations. A strong exothermic step at 227.0 °C corresponds to removal of four pyrazolate anions, which induces a weight loss of 51.84% (calcd. 51.10%). Finally, up to 590.0 °C an elimination of four coordinated chlorine anions as gas Cl_2 causes a weight loss of 9.73% (calcd. 10.29%).

The TG curve of **5** revealed an overall weight loss of 84.63% (calcd. 86.12%) up to 595.0 °C. A weight loss of 33.97% (calcd. 33.35%) was observed during the first two overlapping steps, which is attributed to the elimination of four Et_3NH^+ cations and two NO_3^- anions. The decomposition of four pyrazolate anions took place in an exothermic stage up to 570.0 °C and a weight loss of 42.54% (43.88%) occurred. The remaining 8.12%, which corresponds to removal of four chlorine anions as Cl_2, is in good agreement with the calculated value of 8.89%.

The thermogravimetric analysis of compound **8** revealed an overall weight loss of 78.67% (calcd. 79.57%) over three exothermic stages. A weight loss of 12.47% (calcd. 13.59%) up to 147.0 °C corresponds to removal of two acetate molecules, whereas up to 271.0 °C the weight loss of 21.12% (calcd. 21.68%) is attributed to decomposition and removal of two pyrazole molecules. The elimination of four bridged pyrazolate anions was observed up to 596.0 °C, which induces a weight loss of 45.08% (calcd. 44.30%).

Magnetic Susceptibility Measurements of 2, 4, 5, and 8

General Procedure

After postulating the spin Hamiltonian, the magnetic data were fitted as the integral (orientational) average of the magnetization [Equation (1)].

$$M_{mol} = 1/4\pi \int_0^{2\pi} \int_0^{\pi} M_{a,mol} \sin\theta d\theta d\varphi \quad (1)$$

for different orientations of the magnetic field vector in the spherical coordinates defined as $\mathbf{B}_a = B(\sin\theta\cos\phi, \sin\theta\sin\phi, \cos\theta)$ in order to properly simulate the polycrystalline sample response. The molar magnetization in the a direction of the magnetic field $M_{a,mol}$ was calculated from Equation (2).

$$M_{a,mol} = N_A kT \frac{\partial \ln Z}{\partial B_a} \quad (2)$$

where Z is the partition function resulting from the diagonalization of the complete spin Hamiltonian matrix in the local basis set.[36] The experimental and the calculated temperature dependence of the magnetization at $B = 0.1$ T, transformed to the mean magnetic susceptibility, are plotted as the effective magnetic moment vs. T (Figures 7–10). The goodness of the fit is expressed by using the R factor defined in Equation (3).

$$R = \sum_i \left(M_{cal} - M_{obs}\right)^2 / \sum_i \left(M_{obs}\right)^2 \quad (3)$$

Figure 7 displays the temperature dependence (2–295 K) of the magnetic moment, μ_{eff}, of sample **2**. The effective magnetic moment at $T = 300$ K presents a value of $\mu_{eff} = 5.71\ \mu_B$ and upon cooling remains nearly constant up to 110 K. Below this temperature, its value descends rapidly and at $T = 2.0$ K is equal to $1.45\ \mu_B$. The steep slope of the effective magnetic moment at low temperature reflects the antiferromagnetic exchange between two tetrahedrally coordinated Co^{II} centers with $S_1 = S_2 = 3/2$ as well as the single-ion anisotropy (ZFS). In order to interpret the experimental data, the spin Hamiltonian in Equation (4) was used.

$$\hat{H}_a = -J\left(\mathbf{S}_1 \cdot \mathbf{S}_2\right) + \sum_{i=1}^{2} \mathbf{S}_i \cdot \mathbf{D}_i \cdot \mathbf{S}_i + \mu_B \sum_{i=1}^{2} \mathbf{S}_i \cdot \mathbf{B}_a \cdot \mathbf{g}_i \quad (4)$$

where J is the isotropic exchange constant among adjacent Co^{II} centers and the magnetic anisotropy for Co^{II} is represented by $\boldsymbol{D}_i$ tensors, which are presumed symmetric and traceless, resulting in the axial single-ion ZFS parameter D_i. Due to the identical chromophores of the cobalt centers, $D_1 = D_2 = D$ was applied. The fitting procedure resulted in the following sets of parameters, namely: $J = -6.66\ cm^{-1}$, $g = 2.20$, $D = +8.00\ cm^{-1}$, with R factor equal to 0.0105 (Figure 7). Similar good fit was obtained also with $J = -7.07\ cm^{-1}$, $g = 2.18$, $D = -3.41\ cm^{-1}$, with R factor equal to 0.0214.

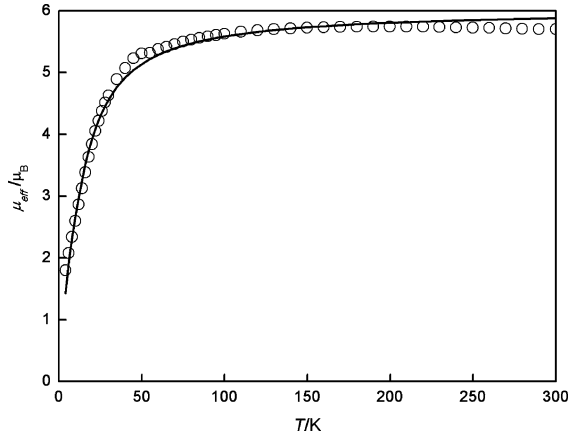

Figure 7. Temperature dependence of the effective magnetic moment for compound **2**: open circles – experimental data; full lines – fitted data.

The effective magnetic moment for mononuclear compound **4** of μ_{eff} = 4.33 μ_B at T = 300 K (Figure 8) remains nearly constant up to 22 K, whereas it decreases monotonically below this temperature until it reaches a value of 3.71 μ_B at T = 2.0 K. The decrease in the effective magnetic moment is attributed to ZFS, and the spin Hamiltonian for S = 3/2 in Equation (5) was used.

$$\hat{H}_a = D\left(\mathbf{S}_z^2 - \mathbf{S}^2/3\right) + \mu_B \mathbf{S}\cdot\mathbf{B}_a\cdot\mathbf{g} \quad (5)$$

The ZFS parameter 2D represents splitting between two Kramers doublets and positive D value means that the ground state is |3/2|, ±1/2>. The fitting procedure resulted in: g = 2.29 and D = +2.05 cm^{-1} with R factor equal to 0.000143 (Figure 8). The value of the ZFS parameter is within the range found in related published work.[37] An attempt to fit the data with a negative D parameter resulted in g = 2.22 and D = –25.9 cm^{-1} with R = 0.0285, but the absolute value of the ZFS parameter, |D|, is too large for tetrahedrally coordinated Co^{II}.

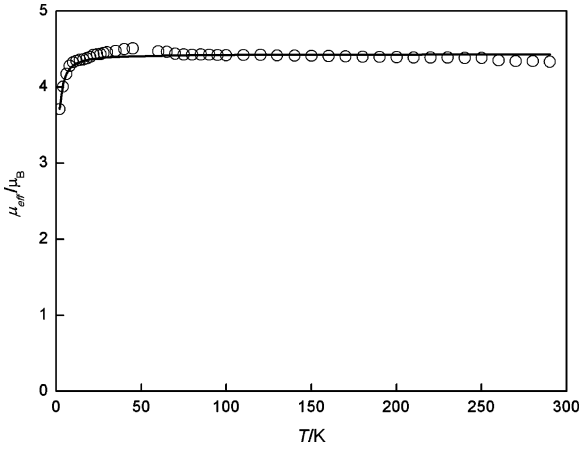

Figure 8. Temperature dependence of the effective magnetic moment for compound **4**: open circles – experimental data; full lines – fitted data.

In the case of compound **5** where two cobalt centers were incorporated, the effective magnetic moment at T = 300 K adopts a value of μ_{eff} = 6.32 μ_B and on cooling remains nearly constant up to 40 K. Below this temperature its value starts to descend and at T = 2.0 K is 4.35 μ_B. The decrease in the effective magnetic moment at low temperature reflects the antiferromagnetic exchange between two tetrahedrally coordinated Co^{II} centers and the value of ZFS as well. Magnetic properties were treated similarly as for compound **2** by using Equation (4).

The fitting procedure resulted in: J = –0.38 cm^{-1}, g = 2.32, and D = +1.22 cm^{-1}, with R factor equal to 0.00957 (Figure 9). An effort to fit the data with a negative D parameter resulted in J = –0.53 cm^{-1}, g = 2.31, and D = –3.47 cm^{-1} with R = 0.0154. Even though the superexchange path is quite long, the two metal centers are weakly antiferromagnetically coupled. This kind of exchange coupling cannot be attributed to intermolecular interaction, as the crystallographically determined distance separating the linear CoPdCo species are longer than 10.5 Å.

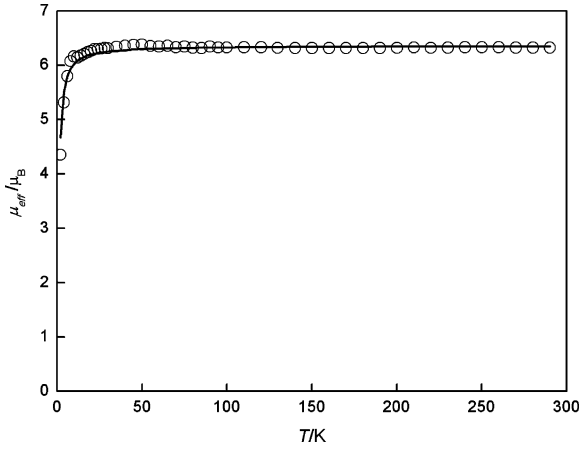

Figure 9. Temperature dependence of the effective magnetic moment for compound **5**: open circles – experimental data; full lines – fitted data.

The effective magnetic moment of compound **8** at T = 300 K revealed a μ_{eff} value of 7.16 μ_B, which upon cooling descends gradually to 3.07 at T = 2.0 K. The magnetic properties of **8** were interpreted by using the spin Hamiltonian for a linear trinuclear species labeled as 1-2-3 [Equation (6)].

$$\hat{H}_a = -J\left(\mathbf{S}_1\cdot\mathbf{S}_2 + \mathbf{S}_2\cdot\mathbf{S}_3\right) + \sum_{i=1}^{3}\mathbf{S}_i\cdot\mathbf{D}_i\cdot\mathbf{S}_i + \mu_B\sum_{i=1}^{3}\mathbf{S}_i\cdot\mathbf{B}_a\cdot\mathbf{g}_i \quad (6)$$

Taking into account the antiferromagnetic exchange among peripheral cobalt centers and the central one, as well as the ZFS term for the peripheral centers with identical chromophores, {CoN_3O}, results in $\mathbf{D}_1 = \mathbf{D}_3$, whereas the ZFS parameter is expected to be zero for the central Co center with a homoleptic chromophore, {CoN_4}, $\mathbf{D}_2 = \mathbf{0}$.

The fitting procedure resulted in J = –6.24 cm^{-1}, g = 2.19, and D = +5.85 cm^{-1} with R factor equal to 0.000121 (Figure 10). We could not obtain a similar fit with a negative D parameter. The Co···Co distances are quite similar

in compounds **1**–**3** and **8**, explaining the similar extend of antiferromagnetic exchange – J values lie in the range of –6.66 to –6.24 for **1**–**3** and **8**. As expected, metal centers are more strongly antiferomagnetically coupled in the case of compounds **1**–**3** and **8** relative to that in compound **5** with J = –0.38 cm^{-1}, because of the longer superexchange path of the latter. On the other hand, the Co_2 and linear Co_3 carboxylate analogues usually reveal significantly weaker antiferromagnetic interactions.[4d,5] A similar magnitude of antiferromagnetic interaction of J = –14.0 cm^{-1} was determined in a trinuclear Co^{II}–carboxylate system in which, however, the distance between six-coordinate Co -centers is by 0.2–0.3 Å shorter than that of **8**, whereas a one-atom μ-O bridge is also present in addition to two μ-RCOO.[5a,38] This suggests that bridging pyrazolate ligands mediate the magnetic exchange between Co^{II} centers quite efficiently. A similar observation was recently reported for systems containing the $Fe_3(\mu_3\text{-O})$-motif.[1]

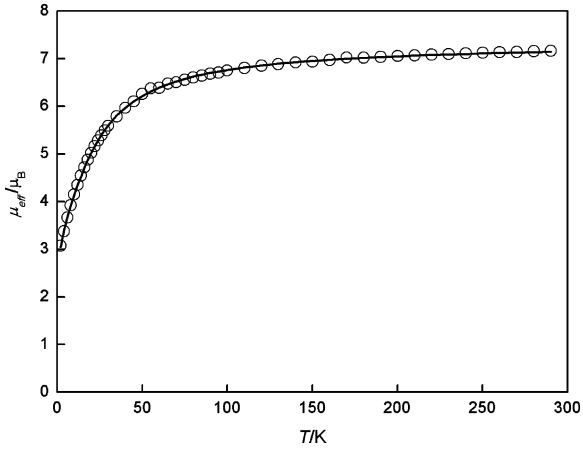

Figure 10. Temperature dependence of the effective magnetic moment for compound **8**: open circles – experimental data; full lines – fitted data.

Conclusions

The syntheses, spectroscopic, crystallographic, and magnetic characterization of a family of dinuclear and linear trinuclear Co/Pd pyrazolate compounds have been reported in this work. The results described here show that pyrazolates are capable of acting efficiently as bridging agents and give rise to stable complexes, not only of cyclic, but linear topologies, as well. The use of bridging pyrazolate ligands promotes efficient magnetic exchange between the metal centers, in comparison to the analogous carboxylate-bridged complexes.

Experimental Section

Physical Measurements: IR spectra of the various compounds dispersed in KBr pellets were recorded with a Nicolet 6700 FTIR spectrometer. Solution electronic absorption spectra were recorded by using 1-cm quartz cells with a Cary 500 UV/Vis/NIR spectrophotometer, whereas reflectance spectra were recorded with a Perkin–Elmer spectrophotometer by using a 1-mm quartz cell. Thermogravimetric analyses (TGA/DTA) were performed with a Thermal Advantage Q500/1000 thermal analysis instrument in the temperature range 25–800 °C under a dinitrogen atmosphere with a heating rate of 5 °C min^{-1}. The temperature dependence of the magnetic susceptibility was measured on polycrystalline powder samples by using a SQUID apparatus (Quantum Design) Magnetometer with an applied field of 0.1 T and a temperature range of 2–300 K. Data were corrected for the sample holder contribution and the underlying diamagnetism of the sample by using Pascal constants.[44]

Syntheses: The synthesis of the ligand 4-X-3,5-Me_2-pzH [X = Cl, Br, I] was performed according to a literature procedure.[45] Commercially available $(NH_4)_2PdCl_4$, $CoCl_2{\cdot}6H_2O$, $Co(NO_3)_2{\cdot}6H_2O$, $Co(CH_3COO)_2{\cdot}4H_2O$,and solvents were used without further purification, unless otherwise reported.

$[Bu_4N]_2[Co_2(4\text{-Cl-}3,5\text{-}Me_2\text{-pz})_2Cl_4]$ (1): A thf solution (15 mL) of $CoCl_2{\cdot}6H_2O$ (0.1 g, 4.2×10^{-4} mol) and 4-Cl-3,5-Me_2-pzH (0.10 g, 7.7×10^{-4} mol) was stirred for 10 min. Upon addition of an excess amount of Et_3N (0.6 mL, 4.3×10^{-3} mol) and solid Bu_4NCl (0.23 g, 8.4×10^{-4} mol), a clear, dark-blue solution resulted. The mixture was filtered and dark-blue crystals of X-ray quality were isolated after 2 d by slow vapor diffusion of diethyl ether into the filtrate. Yield: 0.16 g (65%). $C_{42}H_{84}Br_4Cl_2Co_2N_6$ (1181.55): calcd. C 42.65, H 7.17, N 7.11; found C 42.71, H 7.28, N 7.20.

$[Bu_4N]_2[Co_2(4\text{-Br-}3,5\text{-}Me_2\text{-pz})_2Br_4]$ (2): A thf solution (15 mL) of $CoCl_2{\cdot}6H_2O$ (0.1 g, 4.2×10^{-4} mol) and 4-Br-3,5-Me_2-pzH (0.15 g, 8.4×10^{-4} mol) was stirred for 10 min. Upon addition of an excess amount of Et_3N (0.6 mL, 8.1×10^{-3} mol) and solid Bu_4NCl (0.23 g, 8.3×10^{-4} mol), a clear, dark-blue solution resulted. The mixture was filtered and dark-blue crystals of X-ray quality were isolated after 2 d by slow vapor diffusion of diethyl ether into the filtrate. Yield: 0.18 g (70%). $C_{42}H_{84}Br_6Co_2N_6$ (1270.47): calcd. C 39.71, H 6.66, N 6.62; found C 39.87, H 6.69, N 6.65.

$[Bu_4N]_2[Co_2(4\text{-I-}3,5\text{-}Me_2\text{-pz})_2Cl_4]$ (3): A thf solution (15 mL) of $CoCl_2{\cdot}6H_2O$ (0.1 g, 4.2×10^{-4} mol) and 4-I-3,5-Me_2-pzH (0.18 g, 8.4×10^{-4} mol) was stirred for 10 min. Upon addition of an excess amount of Et_3N (0.6 mL, 4.3×10^{-3} mol) and solid Bu_4NCl (0.23 g, 8.4×10^{-4} mol), a clear, dark-blue solution resulted. The mixture was filtered and dark-blue crystals of X-ray quality were isolated after 2 d by slow vapor diffusion of diethyl ether into the filtrate. Yield: 0.15 g (55%). $C_{42}H_{84}Br_4Co_2I_2N_6$ (1364.45): calcd. C 36.97, H 6.21, N 6.16; found C 37.01, H 6.11, N 6.19.

$[Et_4N]_2[Pd_2Co(4\text{-Br-}3,5\text{-}Me_2\text{-pz})_4Cl_4]$ (4): A thf solution (15 mL) of $CoCl_2{\cdot}6H_2O$ (0.1 g, 4.2×10^{-4} mol) and $(NH_4)_2PdCl_4$ (0.12 g, 4.2×10^{-4} mol) was stirred for 10 min until partial dissolution of $(NH_4)_2PdCl_4$. Addition of solid 4-Br-Me_2-pzH (0.15 g, 8.4×10^{-4} mol), an excess amount of Et_3N (0.6 mL, 8.1×10^{-3} mol), and Et_4NCl (0.23 g, 1.4×10^{-3} mol) was followed by immediate color change of the solution to dark green-blue. The mixture was heated at reflux overnight. Dark-green crystals of X-ray quality were isolated after 3 d by vapor diffusion of diethyl ether into the filtrate. Yield based on Co: 0.29 g (52%). $C_{36}H_{64}Br_4Cl_4CoN_{10}Pd_2$ (1370.14): calcd. C 31.56, H 4.71, N 10.22; found C 31.41, H 4.59, N 10.25.

$[Et_3NH]_4[PdCo_2(4\text{-Br-}3,5\text{-}Me_2\text{-pz})_4Cl_4][NO_3]_2$ (5): A CH_2Cl_2 solution (15 mL) of $Co(NO_3)_2{\cdot}6H_2O$ (0.1 g, 4.2×10^{-4} mol) and $(NH_4)_2PdCl_4$ (0.12 g, 4.2×10^{-4} mol) was stirred for 10 min until partial dissolution of the starting materials. Addition of solid 4-Br-Me_2-pzH (0.22 g, 1.3×10^{-3} mol) and an excess amount of Et_3N (0.6 mL, 8.1×10^{-3}) was followed by immediate color change of the

solution to dark blue. The mixture was heated at reflux overnight. Dark-green block crystals of X-ray quality were isolated after 3 d by vapor diffusion of diethyl ether into the filtrate. Yield based on Co: 0.24 g (72%). $C_{44}H_{88}Br_4Cl_4Co_2N_{14}O_6Pd$ (1594.98): calcd. C 33.13, H 5.56, N 12.29; found C 33.21, H 5.43, N 11.97.

$[Et_3NH]_2[PdCo_2(4\text{-Br-}3,5\text{-}Me_2\text{-pz})_4Cl_4]$ (6): A thf solution (15 mL) of $CoCl_2{\cdot}6H_2O$ (0.1 g, 4.2×10^{-4} mol) and $(NH_4)_2PdCl_4$ (0.12 g, 4.2×10^{-4} mol) was stirred for 10 min until partial dissolution of the starting materials. Addition of solid 4-Br-3,5-Me_2-pzH (0.22 g, 1.3×10^{-3} mol) and an excess amount of Et_3N (0.6 mL, 8.1×10^{-3} mol) was followed by immediate color change of the solution to dark blue. The mixture was heated at reflux overnight. Dark-green crystals of X-ray quality were isolated after 3 d by vapor diffusion of diethyl ether into the filtrate. Yield based on Co: 0.10 g (41%). $C_{56}H_{76}Cl_4Co_2N_{10}Pd$ (1255.33): calcd. C 53.58, H 6.10, N 11.16; found C 53.39, H 6.12, N 11.21.

$[Et_3NH]_2[Pd_3(4\text{-Br-}3,5\text{-}Me_2\text{-pz})_4Cl_4]$ (7): A thf solution (15 mL) of $(NH_4)_2PdCl_4$ (0.12 g, 4.2×10^{-4} mol) was stirred for 10 min until partial dissolution of $(NH_4)_2PdCl_4$. Addition of solid 4-Br-3,5-Me_2-pzH (0.17 g, 9.8×10^{-4} mol) and an excess amount of Et_3N (0.6 mL, 8.1×10^{-3}) was followed by immediate color change of the solution to intense yellow. The mixture was heated at reflux overnight. Yellow block crystals of X-ray quality were isolated after 5 d by vapor diffusion of diethyl ether into the filtrate. Yield: 0.06 g (33%). $C_{32}H_{56}Br_4Cl_4N_{10}Pd_3$ (1361.55): calcd. C 28.23, H 4.15, N 10.29; found C 28.36, H 4.09, N 10.18.

$[Co_3(3,5\text{-}Me_2\text{-pz})_4(3,5\text{-}Me_2\text{-pzH})_2(CH_3CO_2)_2]$ (8): $Co(CH_3COO)_2{\cdot}4H_2O$ (0.1 g, 4.2×10^{-4} mol) was placed in a Schlenk tube and dried in vacuo for 5 d. Solid 3,5-Me_2-pzH (0.08 g, 8.4×10^{-4} mol) was added to the Schlenk tube, and the mixture was heated up to 130 °C under a nitrogen atmosphere for 24 h. The reaction mixture was then heated under reduced pressure to remove acetic acid formed during reaction. The resulting paste was extracted with distilled CH_2Cl_2 to remove unreacted 3,5-Me_2-pzH and then heated at reflux for 24 h. Dark-purple block crystals of X-ray quality were isolated after 4 d by vapor diffusion of diethyl ether into the filtrate. Yield: 0.08 g (70%). $C_{34}H_{50}Co_3N_{12}O_4$ (867.65): calcd. C 47.07, H 5.81, N 19.36; found C 46.96, H 5.70, N 19.45.

X-ray Crystallography: Selected interatomic distances and angles for compounds **1**–**8** are gathered in Tables 1, 2, 3, 4, and 5. Crystal data and details of data collection are listed in Tables 6 and 7. Diffraction data were collected with a Bruker SMART 1 K 3-circle platform diffractometer equipped with a CCD detector at ambient temperature. The frame data were acquired with the SMART[39] software by using Mo-K_α radiation (λ = 0.71073 Å). Final values of the cell parameters were obtained from least-squares refinement of the positions of all observed reflections. The frames were processed by using the SAINT software[40] to give the *hkl* file corrected for Lorentz and polarization effects. The structures were solved by direct method by using the SHELX-97[41] program and refined by least-squares on F^2, SHELXTL-93,[42] incorporated in SHELXTL.[43]

Table 1. Selected interatomic distances (Å) and angles (°) relevant to the coordination sphere of cobalt atoms for compound **1**–**3**.

	1	**2**	**3**
Co1–N1#1	2.002(3)	1.979(9)	1.998(6)
Co1–N2	2.003(3)	2.042(9)	2.003(6)
Co1–Br1	2.4084(7)	2.422(7)	2.413(3)
Co1–Br2	2.4120(6)	2.424(7)	2.420(2)
N1–N2	1.376(4)	1.36(1)	1.373(8)
Co1···Co1#	3.7355(7)	3.707(9)	3.728(2)
N1#1–Co1–N2	107.8(1)	108.4(4)	107.8(2)
N1#1–Co1–Br1	109.22(8)	108.1(3)	109.6(1)
N2–Co1–Br1	111.06(9)	112.9(4)	112.0(2)
N1#1–Co1–Br2	111.29(9)	111.4(4)	110.7(2)
N2–Co1–Br2	110.99(9)	111.3(3)	110.7(2)
Br1–Co1–Br2	106.55(2)	104.7(1)	106.01(5)

Table 2. Selected interatomic distances and angles relevant to the coordination sphere of cobalt atoms for compound **4**.

Bond lengths / Å		Bond angles / °	
Pd2–N3	1.99(1)	N1–Pd2–N3	87.3(1)
Pd2–N1	2.01(1)	N3–Pd2–Cl1	89.6(3)
Pd1–N2	2.01(1)	N2–Pd1–N4	90.5(4)
Pd1–N4	2.04(1)	N7–Pd1–N5	89.4(5)
Co1–N6	2.02(1)	N8–Co1–N6	95.6(5)
Co1–N8	1.99(1)	N8–Co1–Cl4	116.3(4)
Pd1···Pd2	3.407(1)	Pd1–Pd2–Co1	177.96(5)
Pd2···Co1	3.330(2)		

Table 3. Selected interatomic distances (Å) and angles (°) relevant to the coordination sphere of cobalt atoms for compound **5** and **6**.

	5	**6**
Pd1–N3	2.011(4)	2.020(6)
Pd1–N1	2.020(4)	2.014(6)
Co1–N2	1.997(5)	2.047(6)
Co1–N4	2.013(4)	2.020(6)
Co1–Cl2	2.236(2)	2.264(2)
Co1–Cl1	2.277(2)	2.242(2)
N1–N2	1.374(5)	1.370(8)
N3–N4	1.375(5)	1.371(7)
Co1···Pd1	3.415(1)	3.426(1)
Co1···Co1#	6.829(2)	6.853(2)
N3–Pd1–N3#1	180.00(1)	180.0(2)
N3–Pd1–N1	90.9(1)	90.3(2)
N3#1–Pd1–N1	89.0(1)	89.7(2)
N1#1–Pd1–N1	180.0(1)	180.0(2)
Co1–Pd1–Co1#	180.0(1)	180.0(1)
N2–Co1–N4	99.6(2)	104.5(2)
N2–Co1–Cl2	112.1(1)	106.6(2)
N4–Co1–Cl2	116.1(1)	103.8(2)
N2–Co1–Cl1	111.6(1)	112.1(2)
N4–Co1–Cl1	109.7(1)	114.0(2)
Cl2–Co1–Cl1	107.67(9)	114.82(9)

Table 4. Selected interatomic distances and angles relevant to the coordination sphere of cobalt atoms for compound **7**.

Bond lengths / Å		Bond angles / °	
Pd1–N3	2.002(4)	N3–Pd1–N1	88.2(2)
Pd1–N1	2.020(5)	N3–Pd1–Cl2	90.8(1)
Pd2–N2	2.012(4)	N1–Pd1–Cl2	178.7(1)
Pd2–N4	2.017(4)	N2–Pd2–N2#	180.0(3)
Pd1···Pd2	3.3348(6)	N2–Pd2–N4	92.0(1)
Pd1···Pd1#	6.669(1)	N2–Pd2–N4#	87.9(2)
		Pd1–Pd2–Pd3	180.0(1)

Table 5. Selected interatomic distances and angles relevant to the coordination sphere of cobalt atoms for compound **8**.

Bond lengths / Å		Bond angles / °	
Co1–N7	1.991(4)	N7–Co1–N2	121.3(2)
Co1–N2	1.992(4)	N7–Co1–N5	108.0(2)
Co1–N5	1.997(4)	N2–Co1–N5	105.1(1)
Co1–N4	1.997(4)	N7–Co1–N4	105.6(2)
Co2–O1	1.950(4)	N2–Co1–N4	108.6(2)
Co2–N1	2.008(4)	N5–Co1–N4	107.7(2)
Co2–N3	1.980(4)	O1–Co2–N1	99.5(2)
Co2–N9	2.028(4)	N3–Co2–N1	108.5(2)
Co3–O3	1.975(4)	O1–Co2–N9	113.0(2)
Co3–N6	1.990(4)	N3–Co2–N9	107.0(2)
Co3–N8	2.004(4)	N1–Co2–N9	108.1(2)
Co3–N11	2.015(4)	Co1–Co2–Co3	169.10(2)
Co1···Co2	3.609(4)		
Co1···Co3	7.177(1)		

Table 6. Crystallographic data for dinuclear compounds **1**–**3**.

	1	**2**	**3**
Formula	$C_{42}H_{84}Br_6Co_2N_6$	$C_{42}H_{84}Br_4Cl_2Co_2N_6$	$C_{42}H_{84}Br_4Co_2I_2N_6$
M_r	1270.47	1181.55	1364.45
a / Å	12.722(2)	12.64(3)	13.11(2)
b / Å	15.373(2)	15.33(2)	15.80(1)
c / Å	14.613(3)	14.70(4)	14.43(1)
α / °	90	90	90
β / °	90.50(1)	92.4(3)	91.04(7)
γ / °	90	90	90
V / A^3	2857.8(8)	2846(14)	2992(5)
Z	2	2	2
$\rho_{calcd.}$ / Mgm^{-3}	1.476	1.379	1.514
Space group	$P2_1/c$	$P2_1/n$	$P2_1/n$
T / K	298(2)	298(2)	298(2)
λ / Å	0.71073	0.71073	0.71073
μ / mm^{-1}	4.806	3.516	4.286
R_1(final)	0.0339	0.1114	0.0600
wR_2	0.0879	0.2594	0.1693

CCDC-683249 (for **1**), -683250 (for **2**), -683251 (for **3**), -683252 (for **4**), -683253 (for **5**), -683254 (for **6**), -683255 (for **7**), and -683256 (for **8**) contain the supplementary crystallographic data for this paper. These data can be obtained free of charge from The Cambridge Crystallographic Data Centre via www.ccdc.cam.ac.uk/data_request/cif.

Acknowledgments

Work at the University of Puerto Rico has been supported by the National Aeronautics and Space Administration, University Research Center (NASA-URC) (Program No. NCC3-1034) and National Science Foundation (NSF)-Experimental Program to Stimulate Competitive Research (EPSCoR) (Program No. EPS-0223152). R.H. thanks the Czech Ministry of Education, Youth and Sports (Grant No. MSM6198959218).

[1] a) D. Piñero, P. Baran, R. Boca, F. Renz, H. Klein, R. G. Raptis, Y. Sanakis, *Inorg. Chem.* **2007**, *46*, 10981–10989; b) P. Baran, C. Marrero, S. Pérez, R. G. Raptis, *Chem. Commun.* **2002**, 1012–1013.

[2] a) G. Timco, A. Batsanov, F. Larsen, C. Muryn, J. Overgaard, S. Teat, R. Winpenny, *Chem. Commun.* **2005**, 3649–3651; b) D. Albiol, K. Abboud, G. Christou, *Chem. Commun.* **2005**, 4282–4284; c) M. Murugescou, W. Wernsdorfer, K. Abboud, G. Christou, *Angew. Chem. Int. Ed.* **2005**, *44*, 892–896; d) C. Ruiz-Perez, Y. Rodrıguez-Martın, M. Hernandez-Molina, F. S. Delgado, J. Pasan, J. Sanchiz, F. Lloret, M. Julve, *Polyhedron* **2003**, *22*, 2111–2123.

[3] a) S. Midollini, A. Orlandini, P. Rosa, L. Sorace, *Inorg. Chem.* **2005**, *44*, 2060–2066; b) J.-G. Mao, A. Clearfield, *Inorg. Chem.* **2002**, *41*, 2319–2324; c) I. Gil de Muro, F. Mautner, M. Insausti, L. Lezama, M. I. Arriortua, T. Rojo, *Inorg. Chem.* **1998**, *37*, 3243–3251; d) S. G. Ang, B. W. Sun, S. Gao, *Inorg. Chem. Commun.* **2004**, *7*, 795–798; e) X. Zhang, D. Huang, F. Chen, C. Chen, Q. Liu, *Inorg. Chem. Commun.* **2004**, *7*, 662–665.

[4] a) X.-Y. Wang, H.-Y. Wei, Z.-M. Wang, Z.-D. Chen, S. Gao, *Inorg. Chem.* **2005**, *44*, 572–583; b) J. L. Manson, T. Lancaster, L. C. Chapon, S. J. Blundell, J. A. Schlueter, M. L. Brooks, F. L. Pratt, C. L. Nygren, J. S. Qualls, *Inorg. Chem.* **2005**, *44*, 989–995; c) J. Catteric, M. B. Hursthouse, D. New, P. Ornton, *J. Chem. Soc., Chem. Commun.* **1974**, 843–844; d) Y. Oka, K. Inoue, *Chem. Lett.* **2004**, 402–403.

[5] a) R. A. Reynolds, W. R. Dunham, D. Coucouvanis, *Inorg. Chem.* **1998**, *37*, 1232–1241; b) C. E. Sumner Jr, *Inorg. Chem.* **1988**, *27*, 1320–1327; c) D. A. Brown, G. J. Clarkson, N. J. Fitzpatrick, W. K. Glass, A. J. Hussein, T. J. Kemp, H. Meuller-

Table 7. Crystallographic data for trinuclear compounds **4**–**8**.

	4	**5**	**6**	**7**	**8**
Formula	$C_{36}H_{64}Br_4Cl_4CoN_{10}Pd_2$	$C_{44}H_{88}Br_4Cl_4Co_2N_{14}O_6Pd$	$C_{56}H_{76}Cl_4Co_2N_{10}Pd$	$C_{32}H_{56}Br_4Cl_4N_{10}Pd_3$	$C_{34}H_{50}Co_3N_{12}O_4$
M_r	1370.14	1594.98	1255.33	1361.56	867.65
a / Å	11.243(2)	11.031(3)	15.630(5)	11.267(1)	13.376(3)
b / Å	39.357(4)	11.552(4)	11.056(2)	10.010(1)	14.652(5)
c / Å	12.257(3)	14.193(4)	18.962(4)	21.905(3)	21.177(6)
α / °	90	81.76(2)	90	90	90
β / °	109.58(2)	78.23(3)	113.96(2)	103.554(2)	93.37(2)
γ / °	90	84.48(2)	90	90	90
V / A^3	5110(2)	1748.3(8)	2995(1)	2401.6(5)	4143(2)
Z	4	1	2	2	4
$\rho_{calcd.}$ / Mgm^{-3}	1.781	1.515	1.392	1.883	1.391
Space group	$P2_1/c$	$P\bar{1}$	$P2_1/c$	$P2_1/n$	$P2_1/c$
T / K	298(2)	298(2)	298(2)	301(2)	298(2)
λ / Å	0.71073	0.71073	0.71073	0.71073	0.71073
μ / mm^{-1}	4.391	3.210	1.067	4.696	1.237
R_1 (final)	0.0969	0.0528	0.0733	0.0344	0.0647
wR_2	0.2278	0.1113	0.2124	0.0784	0.1276

Bunz, *Inorg. Chem. Commun.* **2004**, *7*, 495–498; d) R. E. P. Winpenny in *Comprehensive Coordination Chemistry* (Eds.: J. A. McCleverty, T. J. Meyers), Pergamon: Oxford, **2004**, vol. 7, ch. 7.3, pp. 125–175; e) R. E. P. Winpenny, *Adv. Inorg. Chem.* **1998**, 1–111; f) Y. Zenga, J. Liub, *Applied Geochem.* **2000**, *15*, 13–25; g) J. Skupiska, *Chem. Rev.* **1991**, *91*, 613–648.

[6] J. Hall, S. Loeb, G. Shimizu, G. Yap, *Angew. Chem. Int. Ed.* **1998**, *37*, 121–123.

[7] a) T. Schalow, B. Brandt, D. Star, M. Laurin, S. Shaikhutdinov, S. Schauermann, J. Libuda, H. Freund, *Angew. Chem. Int. Ed.* **2006**, *45*, 1–6; b) H. Knoezinger, J. Weitcamp, G. Ertl, *Handbook of Heterogeneous Catalysis*, VCH, Weinheim, **1997**; c) J. Thomas, W. Thomas, *Principle and Practice of Heterogeneous Catalysis*, VCH, Weinheim, **1997**.

[8] a) D. Gatteschi, R. Sessoli, *Angew. Chem. Int. Ed.* **2003**, *42*, 268–297 and references cited therein; b) E. M. Rumberger, L. N. Zakharov, A. L. Rheingold, D. N. Hendrickson, *Inorg. Chem.* **2004**, *43*, 6531–6533; c) E. K. Brechin, E. C. Sanudo, W. Wernsdorfer, C. Boskovic, J. Yoo, D. N. Hendrickson, A. Yamaguchi, H. Ishimoto, T. E. Concolino, A. L. Rheingold, G. Christou, *Inorg. Chem.* **2005**, *44*, 502–511; d) P. King, W. Wernsdorfer, K. A. Abboud, G. Christou, *Inorg. Chem.* **2004**, *43*, 7315–7323.

[9] a) H. Oshio, M. Nihei, A. Yoshida, H. Nojiri, M. Nakano, A. Yamaguchi, Y. Karaki, H. Ishimoto, *Chem. Eur. J.* **2005**, *11*, 843–848; b) E. C. Sanudo, W. Wernsdorfer, K. A. Abboud, G. Christou, *Inorg. Chem.* **2004**, *43*, 4137–4144; c) A. J. Wu, J. E. Penner-Hahn, V. L. Pecoraro, *Chem. Rev.* **2004**, *104*, 903–938 and references cited therein; d) K. N. Ferreira, T. M. Iverson, K. Maghlaoui, J. Barber, S. Iwata, *Science* **2004**, *303*, 1831–1838.

[10] a) T. G. St. Pierre, P. Chan, K. R. Bauchspiess, J. Webb, S. Betteridge, S. Walton, D. P. E. Dickson, *Coord. Chem. Rev.* **1996**, *151*, 125–143; b) A. E. Tapper, J. R. Long, R. J. Staples, P. Stavropoulos, *Angew. Chem. Int. Ed.* **2000**, *39*, 2343–2346; c) S. B. Marr, R. O. Carvel, D. T. Richens, H.-J. Lee, M. Lane, P. Stavropoulos, *Inorg. Chem.* **2000**, *39*, 4630–4638; d) K. S. Gavrilenko, T. V. Mypnyuk, V. G. Il′in, S. M. Orlyk, V. V. Pavlishchuk, *Theor. Exp. Chem.* **2002**, *38*, 118–124.

[11] G. La Monica, G. A. Ardizzoia, *Prog. Inorg. Chem.* **1997**, *46*, 151–238.

[12] a) R. Boca, L. Dlhan, G. Mezei, T. Perez, R. G. Raptis, J. Tesler, *Inorg. Chem.* **2003**, *42*, 5801–5803; b) H. V. R. Dias, H. V. K. Diyabalanage, *Polyhedron* **2006**, *25*, 1655–1661; c) G. Yang, R. G. Raptis, *J. Chem. Soc., Dalton Trans.* **2002**, 3936–3938; d) G. Yang, R. G. Raptis, *Inorg. Chem.* **2003**, *42*, 261–263; e) K. Umakoshi, Y. Yamauchi, K. Nakamiya, T. Kojima, M. Yamasaki, H. Kawano, M. Onishi, *Inorg. Chem.* **2003**, *42*, 3907–3916; f) G. Mezei, M. Rivera-Carrillo, R. G. Raptis, *Dalton Trans.* **2007**, 37–40; g) G. Mezei, P. Baran, R. G. Raptis, *Angew. Chem. Int. Ed.* **2004**, *43*, 574–577; h) Y. Zhou, W. Chen, *Organometallics* **2007**, *26*, 2742–2746; i) G. A. Ardizzoia, S. Cenini, G. La Monica, N. Masciocchi, A. Maspero, M. Moret, *Inorg. Chem.* **1998**, *37*, 4284–4292; j) R. G. Raptis, H. H. Murray III, J. P. Fackler Jr, *Inorg. Chem.* **1988**, *27*, 26–33; k) M. Casarin, A. Cingolani, C. De Nicola, D. Falcomer, M. Monari, L. Pandolfo, C. Pettinari, *Cryst. Growth Des.* **2007**, *7*, 676–685.

[13] a) S. Tanase, G. Aromi, E. Bouwman, H. Kooijman, A. Spek, J. Reedijk, *Chem. Commun.* **2005**, 3147–3149; b) S. Nieto, J. Perez, V. Riera, D. Miguel, C. Alvarez, *Chem. Commun.* **2005**, 546–548; c) G. Aromi, A. Bell, S. Teat, A. Whittaker, R. Winpenny, *Chem. Commun.* **2002**, 1896–1897; d) I. Guzei, A. Baboul, G. Yap, A. Rheingold, H. Schlegel, C. Winter, *J. Am. Chem. Soc.* **1997**, *119*, 3387–3388; e) K. Shindo, Y. Mori, K. Motoda, H. Sakiyama, N. Matsumoto, H. Okawa, *Inorg. Chem.* **1992**, *31*, 4987–4993.

[14] a) M. Angaroni, G. A. Ardizzoia, T. Beringhelli, G. La Monica, D. Gatteschi, N. Masciocchi, M. Moret, *J. Chem. Soc., Dalton Trans.* **1990**, 3305–3309; b) K. P. Maresca, J. Zubieta, *Inorg. Chim. Acta* **1997**, *260*, 83–88; c) G. A. Ardizzoia, G. La Monica, A. Maspero, M. Moret, N. Masciocchi, *Eur. J. Inorg. Chem.* **2000**, 181–187; d) H. V. R. Dias, C. S. P. Gamage, *Angew. Chem. Int. Ed.* **2007**, *46*, 2192–2194; e) Q. F. Mokuolu, D. F.-Albiol, L. F. Jones, J. Wolowska, R. M. Kowalczyk, C. A. Kilner, G. Christou, P. C. McGowan, M. A. Halcrow, *Dalton Trans.* **2007**, 1392–1399; f) A. A. Mohamed, A. Burini, R. Galassi, D. Paglialunga, J.-R. G.-Mascaros, K. R. Dunbar, J. P. Fackler Jr, *Inorg. Chem.* **2007**, *46*, 2348–2349.

[15] a) G. A. Ardizzoia, G. La Monica, A. Maspero, M. Moret, N. Masciocchi, *Eur. J. Inorg. Chem.* **2000**, 181–187; b) G. A. Ardizzoia, S. Brenna, G. La Monica, N. Masciocchi, A. Maspero, M. Moret, *Inorg. Chem.* **2001**, *40*, 610–614; c) N. Masciocchi, G. A. Ardizzoia, S. Brenna, G. La Monica, A. Maspero, S. Galli, A. Sironi, *Inorg. Chem.* **2002**, *41*, 6080–6089; d) G. A. Ardizzoia, S. Brenna, S. Cenini, G. La Monica, N. Masciocchi, A. Maspero, *J. Mol. Catal. A* **2003**, *204–205*, 333–340.

[16] a) O. Cador, D. Gatteschi, R. Sessoli, F. Larsen, J. Overgaard, A. Barra, S. Teat, G. Timco, R. Winpenny, *Angew. Chem. Int. Ed.* **2004**, *43*, 5196–5200; b) A. Tasiopoulos, A. Vinslava, W. Wernsdorfer, K. Abboud, G. Christou, *Angew. Chem. Int. Ed.* **2004**, *43*, 2117–2121; c) G. Aromi, A. Batsanov, P. Christian, M. Helliwell, A. Parkin, S. Parsons, A. Smith, G. Timco, R. Winpenny, *Chem. Eur. J.* **2003**, *9*, 5142–5161.

[17] a) A. Tasiopoulos, K. Abboud, G. Christou, *Chem. Commun.* **2003**, 580–581; b) C. Cadiou, R. Coxall, A. Graham, A. Harrison, M. Helliwell, S. Parsons, R. Winpenny, *Chem. Commun.* **2002**, 1106–1107; c) E. Brechin, O. Cador, A. Caneschi, C. Cadiou, S. Harris, S. Parsons, M. Vonci, R. Winpenny, *Chem. Commun.* **2002**, 1860–1861.

[18] a) R. Winpenny, *J. Chem. Soc., Dalton Trans.* **2002**, 1–10; b) E. Brechin, A. Graham, A. Parkin, S. Parsons, A. Seddon, R. Winpenny, *J. Chem. Soc., Dalton Trans.* **2002**, 3242–3252; c) S. Masaoka, S. Furukawa, H. Chang, T. Mizutani, S. Kitagawa, *Angew. Chem. Int. Ed.* **2001**, *40*, 3817–3819.

[19] a) C. Lent, *Science* **2000**, *288*, 1597–1599; b) E. Breuning, M. Ruben, J. Lehn, F. Renz, Y. Garcia, V. Ksenofontov, P. Gütlich, E. Wegelius, K. Rissanen, *Angew. Chem. Int. Ed.* **2000**, *39*, 2504–2507; c) J. M. Lehn, *Angew. Chem. Int. Ed. Engl.* **1990**, *29*, 1304–1319; d) R. H. Holm, P. Kennepohl, E. I. Solomon, *Chem. Rev.* **1996**, *96*, 2239–2314; e) O. Kahn in *Molecular Magnetism*, VCH, Weinheim, Germany, **1993**; f) C. Mirkin, M. Ratner, *Annu. Rev. Phys. Chem.* **1992**, *43*, 719–754; g) J. Stoddart, *Chem. Br.* **1991**, *27*, 714–718; h) A. Becini, D. Gateschi, *EPR of Exchanged Coupled Systems*, Springer, Berlin, **1990**; i) D. Gateschi, O. Kahn, S. Miller (Eds.), *Magnetic Molecular Materials*, NATO ASI Series E, Kluwer Academic, Dordrecht, The Netherlands, **1990**, vol. 198; j) I. Solomon, *Metal Clusters in Proteins* (Ed.: L. Que), American Chemical Society, Washington, DC, **1988**, p. 116; k) E. Hatfield, *Theory and Applications of Molecular Paramagnetism* (Eds.: E. S. Bourdeaux, L. N. Mulay), Wiley, New York, **1976**, p. 350.

[20] a) R. Carroll, C. Gorman, *Angew. Chem. Int. Ed.* **2002**, *41*, 4378–4400; b) P. Anelli, M. Asakawa, P. Ashton, R. Bissel, G. Clavier, R. Gorski, A. Kaifer, S. Langford, G. Mattersteig, S. Menzer, D. Philp, A. Slawin, N. Spencer, J. Stoddart, M. Tolley, D. Williams, *Chem. Eur. J.* **1997**, *3*, 1113–1135; c) R. Balardini, V. Balzani, A. Credi, M. Gadolfi, S. Langford, S. Menzer, L. Prodi, J. Stoddart, M. Venturi, D. Williams, *Angew. Chem. Int. Ed. Engl.* **1996**, *35*, 978–981; d) M. Asakawa, S. Iqbal, J. Stoddart, N. Tinker, *Angew. Chem. Int. Ed. Engl.* **1996**, *35*, 1054–1056; e) [1].-F. Mao, A. Mayr, *Inorg. Chem.* **1996**, *35*, 3183–3187.

[21] S. Kokatam, T. Weyhermuller, E. Bothe, P. Chauduri, K. Wieghart, *Inorg. Chem.* **2005**, *44*, 3709–3717.

[22] P. Chauduri, C. Verani, E. Bill, E. Bothe, T. Weyhermuller, K. Wieghardt, *J. Am. Chem. Soc.* **2001**, *123*, 2213–2223.

[23] H. Chun, C. Verani, P. Chauduri, E. Bothe, E. Bill, T. Weyhermuller, K. Weighart, *Inorg. Chem.* **2001**, *40*, 4157–4166.

[24] D. Burdinski, E. Bill, F. Birckelbach, K. Wieghardt, P. Chauduri, *Inorg. Chem.* **2001**, *40*, 1160–1166.

[25] S. Ross, T. Weyhermuller, E. Bill, K. Wieghardt, P. Chauduri, *Inorg. Chem.* **2001**, *40*, 6656–6665.
[26] D. Burdinski, F. Birckelbach, T. Weyhermuller, U. Florke, H. Haupt, M. Lengen, A. Trautwein, E. Bill, K. Wieghardt, P. Chauduri, *Inorg. Chem.* **1998**, *37*, 1009–1020.
[27] K. Burger, P. Chauduri, K. Wieghardt, *Inorg. Chem.* **1996**, *35*, 2704–2707.
[28] F. Birkelbach, M. Winter, U. Florke, H. Haupt, C. Butzlaff, M. Lengen, E. Bill, A. Trautwein, K. Wieghardt, P. Chauduri, *Inorg. Chem.* **1994**, *33*, 3990–4001.
[29] P. Chauduri, M. Winter, B. Vedova, E. Bill, A. Tautwein, S. Gehring, P. Fleischhauer, B. Nuber, J. Weiss, *Inorg. Chem.* **1991**, *30*, 2148–2157.
[30] U. Florke, H. Haupt, P. Fleischhauer, W. Haase, F. Birkelbach, M. Winter, P. Chauduri, *Inorg. Chem.* **1991**, *30*, 4293–4294.
[31] G. Yang, R. G. Raptis, *J. Chem. Soc., Dalton Trans.* **2002**, 3936–3938.
[32] P. K. Nakamoto, *Infrared and Raman Spectra of Inorganic and Coordination Compounds*, Wiley, New York, **1986**.
[33] F. A. Cotton, G. Wilkinson, *Advance Inorganic Chemistry*, Wiley, New York, **1988**.
[34] a) P. W. Thulstrup, L. Broge, E. Larsen, J. Springborg, *Dalton Trans.* **2003**, 3199–3204; b) M. L. Brader, N. C. Kaarsholm, S. E. Harnung, M. F. Dunn, *J. Biol. Chem.* **1997**, *272*, 1088–1094; c) R. Englman in *The Jahn Teller Effect in Molecules and Crystals*, Wiley, London, **1972**.
[35] a) H. V. A. Briscoe, P. L. Robinson, A. J. Rudge, *J. Chem. Soc.* **1931**, 2211–2213; b) A. Müller, P. Christophliemk, I. Tossidis, *J. Mol. Struct.* **1973**, *15*, 289–299; c) S. Aizawa, S. Iida, K. Matsuda, S. Funahashi, *Inorg. Chem.* **1996**, *35*, 1338–1342; d) L. Chen, F. A. Cotton, *Inorg. Chim. Acta* **1997**, *263*, 9–16; e) N. F. Curtis, O. P. Gladkikh, *Aust. J. Chem.* **2000**, *53*, 727–741.
[36] R. Boča in *Theoretical Foundations of Molecular Magnetism*, Elsevier, Amsterdam, **1999**.
[37] R. Boča, *Coord. Chem. Rev.* **2004**, 757–815.
[38] The reported value of $J = 7\ cm^{-1}$ was determined by using a Hamiltonian of the form $2J(S_1xS_2)$.
[39] *SMART-NT Software Reference Manual* (version 5.059), Bruker AXS, Inc., Madison, WI, **1998**.
[40] *SAINT+ Software Reference Manual* (version 6.02), Bruker AXS, Inc., Madison, WI, **1999**.
[41] G. M. Sheldrick, *SHELXS-97, Program for the Solution of Crystal Structure*, University of Göttingen, Germany, **1997**.
[42] G. M. Sheldrick, *SHELXL-97, Program for the Refinement of Crystal Structure*, University of Göttingen, Germany, **1997**.
[43] *SHELXTL-NT Software Reference Manual* (version 5.1), Bruker AXS, Inc., Madison, WI, **1999**.
[44] E. König in *Landolt-Börstein*, *Neue Serie*, Springer, Berlin, **1966**, vol. 2, p.1–16.
[45] M. K. Ehlert, S. J. Rettig, A. Storr, R. C. Thompson, J. Trotter, *Can. J. Chem.* **1991**, 432–439.

Received: April 4, 2008
Published Online: September 16, 2008

